arXiv:1009.1209v2 [cond-mat.mes-hall] 10 Nov 2010

Polarization Dependence of Raman Spectra in Strained Graphene

Ken-ichi Sasaki*
International Center for Materials Nanoarchitectonics,
National Institute for Materials Science, Namiki, Tsukuba 305-0044, Japan

Katsunori Wakabayashi
International Center for Materials Nanoarchitectonics,
National Institute for Materials Science, Namiki, Tsukuba 305-0044, Japan and
PRESTO, Japan Science and Technology Agency, Kawaguchi 332-0012, Japan

Toshiaki Enoki
Department of Chemistry, Tokyo Institute of Technology, Ookayama, Meguro-ku, Tokyo 152-8551, Japan

(Dated: November 11, 2010)

The polarization dependences of the G, D, and 2D (G′) bands in Raman spectra at graphene bulk and edge are examined theoretically. The 2D and D bands have different selection rules at bulk and edge. At bulk, the 2D band intensity is maximum when the polarization of the scattered light is parallel to that of incident light, whereas the D band intensity does not have a polarization dependence. At edge, the 2D and D bands exhibit a selection rule similar to that of the G band proposed in a previous paper. We suggest that a constraint equation on the axial velocity caused by the graphene edge is essential for the dependence of the G band on the crystallographic orientation observed in the bulk of strained graphene. This is indicative of that the pseudospin and valleyspin in the bulk of graphene can not be completely free from the effect of surrounding edge. The status of the experiments on the G and D bands at the graphene edge is mentioned.

I. INTRODUCTION

Since the early stage of the research on graphene, characterization of a sample has been the central issue and Raman spectroscopy has been playing a major role in characterizing a sample.[1] For example, the 2D (G′) band in Raman spectra is useful in distinguishing a monolayer from few-layer graphene stacked in the Bernal configuration,[2–4] and the appearance of the D band indicates that an intervalley elastic scattering of a photo-excited electron is activated by defect.[5–7] Another advantage of Raman spectroscopy, besides the characterization of a sample, is that Raman spectra can include detailed information on the wave function of the electron.

Raman process concerns with photon, phonon and their mutual interaction through the electrons. Because the electron-photon and electron-phonon interactions in graphene are relevant to pseudospin and valleyspin,[8] the Raman spectra are capable of retrieving information on the pseudospin and valleyspin. An interesting point here is that the pseudospin and valleyspin are sensitive to the presence of graphene edge.[9] As a result, we can have a selection rule specific to the graphene edge. For example, it is known that only the armchair edge enhances the D band intensity and that the intensity depends on the angle between the armchair edge and the polarization of incident (scattered) laser light.[10–12]

In a previous paper, we proposed a selection rule for the G band.[13,14] This selection rule states, for example, that the Raman intensity is enhanced when the polarization of Raman laser is parallel (perpendicular) to the armchair (zigzag) edge. This prediction has been supported by recent experiments of Cong *et al.*[15] and Begliarbekov *et al.*[16] Their experiments illustrate that the G band intensity exhibits the anomalous polarization dependence at graphene edges which is different from the polarization dependence at the interior (bulk). Their results could be naturally explained in terms of the special behavior of the pseudospin and valleyspin near the edges of graphene.

In this paper, we explore selection rules for the D and 2D (G′) bands at bulk and edge. Since the 2D band is a prominent peak in Raman spectra, the selection rule must be useful in extracting more information on the pseudospin and valleyspin from the Raman spectra. In addition, we examine the G band in strained graphene as the application of the selection rule for the G band. It is known that strain splits the G band into two subbands called G^+ and G^-, and that the Raman intensity of each subband has a crystallographic orientation dependence.[17,18] Our result suggests that the crystallographic orientation dependence observed in the bulk of strained graphene is relevant to the selection rule of the G band for the graphene edge. The pseudospin and valleyspin in the bulk of graphene seem to be not completely free from the effect of surrounding edge.

This paper is organized as follows. In Sec. II we derive the selection rule of the G band for the graphene edge in a unified manner. In Sec. III we apply the constraint which is essential for the selection rule of the G band to explaining the crystallographic orientation dependence of the G band Raman intensity observed in strained graphene. The selection rules of the D and 2D bands are proposed in Sec. IV. Discussion and summary are given in Sec. V.

II. QUICK OVERVIEW OF SELECTION RULE FOR G BAND

In this section we reproduce the selection rule of the G band for the graphene edge obtained in a previous paper,[14] by employing an approach based on two velocities associated with the gauge fields for photon and phonon. This new approach can help us to recognize strange similarity between the zigzag and armchair edges. This similarity is represented by the condition Eq. (11) or Eq. (16). As we will show in Sec. III, this condition is necessary to explain recent experiments showing that the G band exhibits a polarization dependence on the crystallographic orientation of strained graphene.[17,18]

A. Two Velocities

Let us begin with the Hamiltonian including photon field $\mathbf{A}$ and phonon fields $\mathbf{A}^{\rm q}$ and ϕ,[8]

$$H = \begin{pmatrix} \boldsymbol{\sigma}\cdot(\hat{\mathbf{p}} - e\mathbf{A} + \mathbf{A}^{\rm q}) & \phi\sigma_x \\ \phi^*\sigma_x & \boldsymbol{\sigma}'\cdot(\hat{\mathbf{p}} - e\mathbf{A} - \mathbf{A}^{\rm q}) \end{pmatrix}, \quad (1)$$

where $\hat{\mathbf{p}} = -i\nabla$ is the momentum operator, σ_a $(a = 0, x, y, z)$ is the pseudospin, $\boldsymbol{\sigma} \equiv (\sigma_x, \sigma_y)$, and $\boldsymbol{\sigma}' \equiv (-\sigma_x, \sigma_y)$. The phonon field ϕ $(\mathbf{A}^{\rm q})$ gives rise to an intervalley (intravalley) scattering. In Eq. (1), we have adopted units in which $\hbar = 1$ and $v_{\rm F} = 1$, and omitted the position dependence in the variables $\mathbf{A}^{\rm q}$ and ϕ because we are interested in the Γ and K points phonon modes.

From Eq. (1), we define two velocity operators, $\boldsymbol{v}$ and $\boldsymbol{v}^{\rm q}$, as follows:

$$\begin{aligned} \boldsymbol{v} &\equiv -\frac{1}{e}\frac{\partial H}{\partial \mathbf{A}} = \begin{pmatrix} \boldsymbol{\sigma} & 0 \\ 0 & \boldsymbol{\sigma}' \end{pmatrix}, \\ \boldsymbol{v}^{\rm q} &\equiv \frac{\partial H}{\partial \mathbf{A}^{\rm q}} = \begin{pmatrix} \boldsymbol{\sigma} & 0 \\ 0 & -\boldsymbol{\sigma}' \end{pmatrix}. \end{aligned} \quad (2)$$

The operator $\boldsymbol{v}$ is nothing but the usual velocity operator that couples to an electro-magnetic gauge field $\mathbf{A}$. Note that an electromagnetic current is given by multiplying $-ev_{\rm F}$ and $\boldsymbol{v}$ together, and the unperturbed Hamiltonian is written as $H_0 = \boldsymbol{v}\cdot\hat{\mathbf{p}}$. The velocity $\boldsymbol{v}^{\rm q}$ is distinct from $\boldsymbol{v}$ for the sign in front of $\boldsymbol{\sigma}'$. It may be appropriate to call $\boldsymbol{v}^{\rm q}$ an axial velocity because $\boldsymbol{v}^{\rm q}$ has some analogy to the axial current in quantum electrodynamics. In graphene, the axial velocity $\boldsymbol{v}^{\rm q}$ couples with a lattice deformation. Note that phonon is one example of a lattice deformation and a general lattice deformation such as ripples and edges can be represented by an axial gauge field $\mathbf{A}^{\rm q}(\mathbf{r})$.[19–21]

By using τ_a $(a = 0, x, y, z)$ to represent the valleyspin, we write the component of the velocity $\boldsymbol{v}$ as

$$\begin{aligned} v_x &= \sigma_x\tau_z, \\ v_y &= \sigma_y\tau_0, \end{aligned} \quad (3)$$

and that of $\boldsymbol{v}^{\rm q}$ as

$$\begin{aligned} v^{\rm q}_x &= \sigma_x\tau_0, \\ v^{\rm q}_y &= \sigma_y\tau_z. \end{aligned} \quad (4)$$

Note that these two velocities $\boldsymbol{v}$ and $\boldsymbol{v}^{\rm q}$ are related with each other via the pseudospin σ_z as

$$v_i\sigma_z = -i\epsilon_{ij}v^{\rm q}_j, \quad (5)$$

where $i, j \in \{x, y\}$ and ϵ_{ij} is antisymmetric tensor satisfying $\epsilon_{xy} = 1$, $\epsilon_{yx} = -1$, and $\epsilon_{xx} = \epsilon_{yy} = 0$. In the following subsections, by examining the effect of the zigzag and armchair edges on the two velocities $\boldsymbol{v}$ and $\boldsymbol{v}^{\rm q}$, we derive the selection rule for the G band.

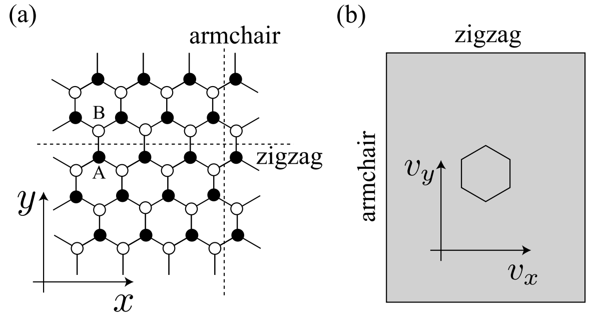

FIG. 1: (a) The coordinate system represents the crystal reference system. The zigzag edge is parallel to the x-axis, while the armchair edge is parallel to the y-axis. (b) A graphene system with rectangle shape enclosed by the zigzag and armchair edges.

B. Zigzag Edge

First of all, the electronic velocity $\boldsymbol{v}$ normal to the zigzag edge must vanish.[22,23] By taking the zigzag edge along the x-axis [see Fig. 1(a)], we thus have the condition

$$\langle v_y \rangle = 0. \quad (6)$$

Here, $\langle \mathcal{O} \rangle$ denotes the expectation value of the operator $\mathcal{O}$ with respect to the standing wave near the edge. A general wave function can be represented by

$$\Psi(\mathbf{r}) = \begin{pmatrix} \Psi_{\rm K}(\mathbf{r}) \\ \Psi_{\rm K'}(\mathbf{r}) \end{pmatrix}, \quad (7)$$

where $\Psi_{\rm K}(\mathbf{r})$ $[\Psi_{\rm K'}(\mathbf{r})]$ is the two-component wave function for an electron near the K [K′] point. The two-component structure corresponds to the pseudospin. Note that the zigzag edge is not the source of intervalley scattering.[14,24] As a result, the standing wave near the zigzag edge is written as

$$\Psi(\mathbf{r}) = \begin{pmatrix} \Psi_{\rm K}(\mathbf{r}) \\ 0 \end{pmatrix}, \quad \text{or} \quad \Psi(\mathbf{r}) = \begin{pmatrix} 0 \\ \Psi_{\rm K'}(\mathbf{r}) \end{pmatrix}. \quad (8)$$

Thus, Eq. (6) leads to

$$\begin{aligned}&\int_S \Psi_{\rm K}^\dagger(\mathbf{r})\sigma_y\Psi_{\rm K}(\mathbf{r})dxdy = 0,\\&\int_S \Psi_{\rm K'}^\dagger(\mathbf{r})\sigma_y\Psi_{\rm K'}(\mathbf{r})dxdy = 0.\end{aligned}\tag{9}$$

Namely, the condition $\langle v_y\rangle = 0$ must be satisfied independently for the K and K′ points. Because

$$\begin{aligned}(\tau_0+\tau_z)\Psi(\mathbf{r}) &= 2\begin{pmatrix}\Psi_{\rm K}(\mathbf{r})\\0\end{pmatrix},\\(\tau_0-\tau_z)\Psi(\mathbf{r}) &= 2\begin{pmatrix}0\\\Psi_{\rm K'}(\mathbf{r})\end{pmatrix},\end{aligned}\tag{10}$$

Eq. (9) is possible only when $\langle\sigma_y(\tau_0\pm\tau_z)\rangle = 0$ [i.e., $\langle v_y\rangle \pm \langle v_y^{\rm q}\rangle = 0$] is also satisfied. Hence, we get a constraint for the axial velocity as

$$\langle v_y^{\rm q}\rangle = 0.\tag{11}$$

We will show below that the selection rule for the G band arises from the two conditions given by Eqs. (6) and (11).

The Hamiltonian contains the electron-phonon (el-ph) interaction, $\mathbf{A}^{\rm q}\cdot\boldsymbol{v}^{\rm q}$, and the constraint Eq. (11) shows that $A_y^{\rm q}$ component does not have a nonzero el-ph matrix element. Because the vector $\mathbf{A}^{\rm q}$ is pointing perpendicular to the optical phonon eigen vector,[14,25,26] $A_y^{\rm q}$ component corresponds to the optical phonon mode whose displacement vector is parallel to the zigzag edge, u_x, which we called the longitudinal optical (LO) phonon mode in a previous paper.[13,14] Thus, Eq. (11) shows that the LO mode is not a Raman active mode near the zigzag edge.[48] Only transverse optical (TO) phonon mode $A_x^{\rm q}$ (u_y) can be Raman active.

Moreover, since the pseudospin σ_z changes the wave function from symmetric (bonding) to anti-symmetric (anti-bonding), the optical transition amplitude is proportional to the expectation value of $\boldsymbol{v}\sigma_z$. The optical transition does not take place when the polarization of the incident (or scattered) laser light is parallel to the zigzag edge (or the x-axis) because the corresponding optical matrix element vanishes as

$$A_x\langle v_x\sigma_z\rangle = -iA_x\langle\sigma_y\tau_z\rangle = -iA_x\langle v_y^{\rm q}\rangle = 0,\tag{12}$$

due to Eq. (11). Similarly, the phonon softening (Kohn anomaly) is relevant to the expectation value of $\boldsymbol{v}^{\rm q}\sigma_z$. The phonon softening is absent for the unique Raman active TO ($A_x^{\rm q}$) mode because

$$A_x^{\rm q}\langle v_x^{\rm q}\sigma_z\rangle = -iA_x^{\rm q}\langle v_y\rangle = 0,\tag{13}$$

due to Eq. (6). Note that the LO mode ($A_y^{\rm q}$) can undergo a phonon softening effect, however, the LO mode is invisible to Raman spectra.

In summary, the polarization of the laser light should be perpendicular to the zigzag edge in order to have a Raman intensity, and the corresponding Raman active mode is the TO mode which is free from the phonon softening effect. It is important to recognize that this selection rule is a consequence of the conditions Eqs. (6) and (11) for the electronic and axial velocities.

C. Armchair Edge

The armchair edge can be examined in a manner similar to that for the zigzag edge. The electronic velocity normal to the armchair edge must vanish. By taking the armchair edge along the y-axis (see Fig. 1(a)), we have the condition

$$\langle v_x\rangle = 0.\tag{14}$$

Note that the armchair edge is not the source of intravalley scattering and preserves the pseudospin under an intervalley scattering.[14,24] As a result, we obtain $(i = x, y)$

$$\int_S \Psi_{\rm K}^\dagger(\mathbf{r})\sigma_i\Psi_{\rm K}(\mathbf{r})dxdy = \int_S \Psi_{\rm K'}^\dagger(\mathbf{r})\sigma_i\Psi_{\rm K'}(\mathbf{r})dxdy.\tag{15}$$

This equation is equivalent to the conditions $\langle\sigma_x\tau_z\rangle = 0$ and $\langle\sigma_y\tau_z\rangle = 0$. The former condition $\langle\sigma_x\tau_z\rangle = 0$ is nothing but Eq. (14), while the latter one $\langle\sigma_y\tau_z\rangle = 0$ corresponds to

$$\langle v_y^{\rm q}\rangle = 0.\tag{16}$$

From this condition it is straightforward to show that only the LO mode $A_x^{\rm q}$ (u_y) is Raman active mode at the armchair edge. The optical transition does not take place when the polarization of the incident laser light is perpendicular to the armchair edge because

$$A_x\langle v_x\sigma_z\rangle = -iA_x\langle v_y^{\rm q}\rangle = 0,\tag{17}$$

due to Eq. (16). Furthermore, we see by using Eq. (14) that the Raman inactive TO mode ($A_y^{\rm q}$) does not undergo the phonon softening because

$$A_y^{\rm q}\langle v_y^{\rm q}\sigma_z\rangle = iA_y^{\rm q}\langle v_x\rangle = 0.\tag{18}$$

The Raman active LO mode ($A_x^{\rm q}$) can exhibit a phonon softening effect. To summarize the selection rule of the G band for the armchair edge, the polarization of the laser light should be parallel to the armchair edge in order to have a Raman intensity, and the corresponding Raman active mode is the LO mode which undergoes a phonon softening effect.

The zigzag and armchair edges are distinct concerning the usual velocity $\boldsymbol{v}$ as $\langle v_y\rangle = 0$ and $\langle v_x\rangle = 0$, respectively. Note, however, that the zigzag and armchair edges are not distinct with respect to the axial velocity $\boldsymbol{v}^{\rm q}$. The constraint for the axial velocity at the armchair edge is the same as that at the zigzag edge as shown by Eqs. (11) and (16), although the origins of Eqs. (11) and (16) are totally different. For the zigzag edge, Eq. (11) is satisfied both for the K and K′ points since the zigzag edge is not the source of an intervalley scattering. In other words, the zigzag edge affects only the pseudospin as $\langle\sigma_y\rangle = 0$.[14] The zigzag edge is irrelevant to the valleyspin. In contrast, Eq. (16) is satisfied because the armchair edge is the source of an intervalley scattering and preserves the pseudospin. The armchair edge affects only the valleyspin and is irrelevant to the pseudospin.

III. UNIAXIAL STRAIN

In this section we apply the selection rule of the G band for graphene edge to the G band in strained graphene. It is known that strain lifts the degeneracy of the G band, so that the G band splits into two subbands called G^+ and G^-. The eigenvectors for the atomic displacements are perpendicular to the direction of strain for the G^+ mode, and parallel to the G^- mode.[17,18] By defining $\mathbf{A}^\text{q}_+$ ($\mathbf{A}^\text{q}_-$) field for the G^+ (G^-) mode, we see that $\mathbf{A}^\text{q}_+$ is parallel to the direction of strain, while $\mathbf{A}^\text{q}_-$ is perpendicular to it since $\mathbf{A}^\text{q}$ is pointing perpendicular to the corresponding optical phonon eigenvector. Recent experiments by Huang *et al.*[17] and Mohiuddin *et al.*[18] for bulk of strained graphene show that the Raman intensity of each G^+ and G^- mode has the crystallographic orientation dependence. We suggest that the crystallographic orientation dependence of the G band Raman intensity observed at bulk can be attributed to the constraint $\langle v^\text{q}_y\rangle = 0$ obtained in the previous section for the graphene edge. The difference between the bulk and edge is pointed out with respect to the crystallographic orientation dependence of the G band Raman intensity and Kohn anomaly effect.

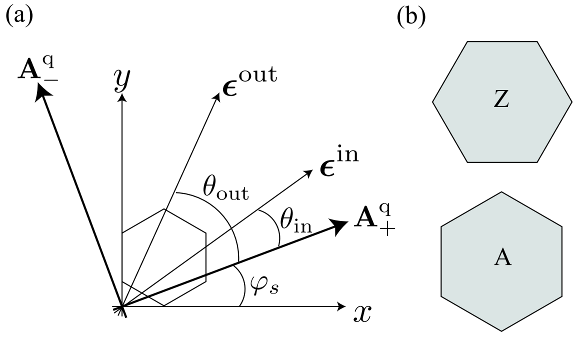

FIG. 2: (a) The strain is at the angle φ_s with respect to the x-axis. The direction of strain is parallel to $\mathbf{A}^\text{q}_+$. The angle between the strain and the incident (scattered) laser polarization is denoted by θ_in (θ_out). The axial vector $\mathbf{A}^\text{q}_+$ corresponds to the G^+ mode, while $\mathbf{A}^\text{q}_-$ corresponds to the G^- mode. (b) A hexagonal graphene with zigzag edges (top), and that with armchair edges (bottom).

A. Bulk

Since the polarization of light, $\boldsymbol{\epsilon}$, is parallel to $\mathbf{A}$, the electron-photon interaction, $\mathbf{A}\cdot\boldsymbol{v}$, is proportional to $\boldsymbol{\epsilon}\cdot\boldsymbol{v}$. Let the polarizations of incident light and scattered light be $\boldsymbol{\epsilon}^\text{in}$ and $\boldsymbol{\epsilon}^\text{out}$, respectively. Then the effective photon-phonon interaction for the phonon mode $\mathbf{A}^\text{q}$ is given by

$$\mathcal{H}_\text{G} \equiv e^2(\boldsymbol{\epsilon}^\text{out}\cdot\boldsymbol{v}\sigma_z)^\dagger(\mathbf{A}^\text{q}\cdot\boldsymbol{v}^\text{q})(\boldsymbol{\epsilon}^\text{in}\cdot\boldsymbol{v}\sigma_z). \tag{19}$$

Here, we have omitted to write the electron propagator by assuming a resonance Raman process, in which the photo-excited electron is a resonant state. Note that this effective interaction is for the bulk where the electron propagator does not depend on the pseudospin. Owing to Eq. (5), $\mathcal{H}_\text{G}$ can be expressed in terms of the axial velocity operator only. Moreover, by using the properties of the axial velocity operator, $v^\text{q}_i v^\text{q}_i = \sigma_0\tau_0$ $(i = x, y)$ and $v^\text{q}_x v^\text{q}_y = -v^\text{q}_y v^\text{q}_x$, we rewrite $\mathcal{H}_\text{G}$ in the form[49]

$$\begin{aligned}\frac{\mathcal{H}_\text{G}}{e^2} &= (\epsilon^\text{in}_x\epsilon^\text{out}_x - \epsilon^\text{in}_y\epsilon^\text{out}_y)(-A^\text{q}_x v^\text{q}_x + A^\text{q}_y v^\text{q}_y)\\ &\quad - (\epsilon^\text{in}_x\epsilon^\text{out}_y + \epsilon^\text{in}_y\epsilon^\text{out}_x)(A^\text{q}_x v^\text{q}_y + A^\text{q}_y v^\text{q}_x).\end{aligned} \tag{20}$$

Note that $\mathcal{H}_\text{G}$ is linear in v^q_i. This feature is unique to the G band and is not seen in the case of the D and 2D bands as we will show later. By introducing the angles, θ_in, θ_out, and φ_s as shown in Fig. 2, one has $\epsilon^\text{in}_x = \epsilon^\text{in}\cos(\theta_\text{in}+\varphi_s)$, $\epsilon^\text{in}_y = \epsilon^\text{in}\sin(\theta_\text{in}+\varphi_s)$, $\epsilon^\text{out}_x = \epsilon^\text{out}\cos(\theta_\text{out}+\varphi_s)$, $\epsilon^\text{out}_y = \epsilon^\text{out}\sin(\theta_\text{out}+\varphi_s)$, and

$$\begin{aligned}A^\text{q}_x &= A^\text{q}_+\cos\varphi_s - A^\text{q}_-\sin\varphi_s,\\ A^\text{q}_y &= A^\text{q}_+\sin\varphi_s + A^\text{q}_-\cos\varphi_s.\end{aligned} \tag{21}$$

By putting these into Eq. (20), we get

$$\begin{aligned}\frac{\mathcal{H}_\text{G}}{e^2\epsilon^\text{in}\epsilon^\text{out}} &= -\,(v^\text{q}_x A^\text{q}_+ - v^\text{q}_y A^\text{q}_-)\cos(\theta_\text{in}+\theta_\text{out}+\varphi_s)\\ &\quad -\,(v^\text{q}_y A^\text{q}_+ + v^\text{q}_x A^\text{q}_-)\sin(\theta_\text{in}+\theta_\text{out}+\varphi_s).\end{aligned} \tag{22}$$

The probability amplitude of the process is given by the expectation value $\langle\mathcal{H}_\text{G}\rangle$, and the Raman intensity of the A^q_+ (A^q_-) mode is given by the square of the coefficient of A^q_+ (A^q_-) in $\langle\mathcal{H}_\text{G}\rangle$ as

$$\begin{aligned}I_{\text{G}^+} &\propto |\langle v^\text{q}_x\rangle\cos(\Psi) + \langle v^\text{q}_y\rangle\sin(\Psi)|^2,\\ I_{\text{G}^-} &\propto |\langle v^\text{q}_y\rangle\cos(\Psi) - \langle v^\text{q}_x\rangle\sin(\Psi)|^2,\end{aligned} \tag{23}$$

where we have defined $\Psi \equiv \theta_\text{in}+\theta_\text{out}+\varphi_s$.[50]

It is important to recognize that only when $\langle v^\text{q}_y\rangle = 0$, I_{G^+} and I_{G^-} can have the crystallographic orientation dependence of the Raman intensity:

$$\begin{aligned}I_{\text{G}^+} &\propto \cos^2(\Psi),\\ I_{\text{G}^-} &\propto \sin^2(\Psi),\end{aligned} \tag{24}$$

which were used to fit the observed polarization dependence of the Raman intensity on the crystallographic orientation in strained graphene.[17,18] Note that without some constraint for $\boldsymbol{v}^\text{q}$, the Raman intensity cannot have a crystallographic orientation dependence since the electronic dispersion is isotropic about the Dirac point.[51] The wave function in a periodic graphene does not yield a constraint for the axial velocity $\boldsymbol{v}^\text{q}$, so that not only $\langle v^\text{q}_x\rangle$ but also $\langle v^\text{q}_y\rangle$ can take a nonzero value. In this case, we can have $\langle v^\text{q}_x\rangle = \cos\theta(\mathbf{k})$ and $\langle v^\text{q}_y\rangle = \sin\theta(\mathbf{k})$, where $\theta(\mathbf{k})$ is the angle between the wave vector $\mathbf{k}$ and the k_x-axis. After the integral over the variable $\theta(\mathbf{k})$, the intensity becomes independent of the angle Ψ. Since we have the constraint $\langle v^\text{q}_y\rangle = 0$ for both the zigzag and armchair orientations, it is naturally expected for the graphene sample with rectangle shape enclosed by zigzag and armchair edges shown in Fig. 1(b) that we still have $\langle v_y^{\rm q}\rangle = 0$, and that only $\langle v_x^{\rm q}\rangle$ can have a non-vanishing value. Then we can reproduce the crystallographic orientation dependence. As a matter of course, there remains a question of whether or not the constraint $\langle v_y^{\rm q}\rangle = 0$ holds in a graphene sample with a general edge shape. A further discussion on this point will be given in Sec. V.

If the Raman intensity of the G band in the bulk of graphene does not have a polarization dependence, there are in principle two ways to interpret this. One way is to assume that the bulk of graphene with edge is identical to the "bulk" of a periodic graphene without edge. In this case both $I_{\rm G^+}$ and $I_{\rm G^-}$ do not have any polarization dependence. The other way is to assume that the existence of graphene edge gives rise to some constraint for the axial velocity in the "bulk" like $\langle v_y^{\rm q}\rangle = 0$ with respect to the states participating in the Raman process. In this case both $I_{\rm G^+}$ and $I_{\rm G^-}$ do have polarization dependence, but the sum of them $I_{\rm G^+} + I_{\rm G^-}$ does not. Thus, without strain, the two kinds of "bulk" can not be distinct. The experimental results[17,18] in the bulk of strained graphene indicate that the later interpretation is plausible.

B. Edge

We now examine the Raman intensity of the $\rm G^+$ mode and that of $\rm G^-$ mode for the graphene edge. Since we have the constraint $\langle v_y^{\rm q}\rangle = 0$ for the standing wave, we need to modify Eq. (19) at the graphene edge as

$$\langle \mathcal{H}'_{\rm G}\rangle \equiv e^2 \langle(\boldsymbol{\epsilon}^{\rm out}\cdot \boldsymbol{v}\sigma_z)^\dagger\rangle \langle \mathbf{A}^{\rm q}\cdot \boldsymbol{v}^{\rm q}\rangle \langle \boldsymbol{\epsilon}^{\rm in}\cdot \boldsymbol{v}\sigma_z\rangle. \tag{25}$$

In contrast to the effective interaction for the bulk given in Eq. (19), each interaction operator is replaced with the expectation value of the operator, by which the intermediate state can satisfy the constraint for the standing wave. Physically speaking, this modification assumes that the coherence between ingoing and outgoing states of the standing wave is strong, so that the intermediate state can not transfer into an ingoing state or an outgoing state independently. This coherence may be weak in the bulk, for which case Eq. (19) would become a better approximation. We note that regardless of the weakness of the coherence in the bulk, the coherence for the initial and final states in the Raman process can lead to the crystallographic orientation dependences of the $\rm G^+$ and $\rm G^-$ bands.

Now, with the constraint $\langle v_y^{\rm q}\rangle = 0$, Eq. (25) becomes

$$\langle \mathcal{H}'_{\rm G}\rangle = e^2 A_x^{\rm q} \epsilon_y^{\rm out} \epsilon_y^{\rm in} \langle v_x^{\rm q}\rangle^3. \tag{26}$$

This is a mathematical expression of the selection rule for the G band near the graphene edge in shortened form. Since $\epsilon_y^{\rm in} = \epsilon^{\rm in}\sin(\theta_{\rm in}+\varphi_s)$, and $\epsilon_y^{\rm out} = \epsilon^{\rm out}\sin(\theta_{\rm out}+\varphi_s)$ (see Fig. 2), we have with Eq. (21) that $\langle \mathcal{H}'_{\rm G}\rangle \propto (A_+^{\rm q}\cos\varphi_s - A_-^{\rm q}\sin\varphi_s)\sin(\theta_{\rm in}+\varphi_s)\sin(\theta_{\rm out}+\varphi_s)$. From the coefficients of $A_+^{\rm q}$ and $A_-^{\rm q}$ in this representation, the Raman intensity of each mode is given by

$$\begin{aligned} I_{\rm G^+} &\propto \cos^2(\varphi_s)\sin^2(\theta_{\rm in}+\varphi_s)\sin^2(\theta_{\rm out}+\varphi_s), \\ I_{\rm G^-} &\propto \sin^2(\varphi_s)\sin^2(\theta_{\rm in}+\varphi_s)\sin^2(\theta_{\rm out}+\varphi_s). \end{aligned} \tag{27}$$

It is amusing to note that $I_{\rm G^-}$ ($I_{\rm G^+}$) vanishes when $\varphi_s = 0$ ($\varphi_s = 90°$). Note also that the ratio $I_{\rm G^-}/I_{\rm G^+}$ depends only on the angle φ_s, which is in contrast to the case of the bulk.

C. Kohn Anomaly Effect

Kohn anomaly effect is useful for illuminating the essential difference between the predictions of the two models for the bulk and edge [Eqs. (19) and (25)]. For the G band, the Kohn anomaly effect is caused by the electron-hole pair creation from the phonon which is described as a vertical transition in the picture of the Dirac cone.[27–29] The probability amplitude for the vertical pair creation from a phonon mode $\mathbf{A}^{\rm q}$ is given by

$$M_{\rm G} = \langle (\mathbf{A}^{\rm q}\cdot \boldsymbol{v}^{\rm q}\sigma_z)^\dagger (\mathbf{A}^{\rm q}\cdot \boldsymbol{v}^{\rm q}\sigma_z)\rangle \tag{28}$$

This is the formula for the bulk where we assume that the "spin" (pseudospin and valleyspin) of the intermediate state can be arbitrary (See Fig. 3). In other words, the propagator of electron in the bulk is proportional to the identity matrix. In this case, regardless of the character of the initial state, we obtain $M_{\rm G} = \mathbf{A}^{\rm q}\cdot\mathbf{A}^{\rm q}$ from Eq. (28). This means that both the LO and TO modes in the bulk undergo the Kohn anomaly effect. On the other hand, the corresponding matrix element for the edge is given by

$$M'_{\rm G} = \langle (\mathbf{A}^{\rm q}\cdot \boldsymbol{v}^{\rm q}\sigma_z)^\dagger\rangle \langle \mathbf{A}^{\rm q}\cdot \boldsymbol{v}^{\rm q}\sigma_z\rangle. \tag{29}$$

For the case of edge, we assume that the intermediate state is given by the standing wave which has the constraint condition for the "spin". It is easy to show that $M'_{\rm G} = (\mathbf{A}^{\rm q}\times\langle \boldsymbol{v}\rangle)^2$. This leads to the selection rule for the G band at edge since we have $\langle v_y^{\rm q}\rangle = 0$. This is the cause of the asymmetry that only the LO mode can undergo the Kohn anomaly effect at both the zigzag and armchair edges.[13,14]

IV. D AND 2D BANDS

In this section we study the polarization dependences of the Raman intensities of the D and 2D (G′) bands for the bulk and edge. It is shown that the Raman intensity of the D band in the bulk does not have a polarization dependence, while that of the 2D band in the bulk can have the polarization dependence, $I_{\rm 2D} \propto (\boldsymbol{\epsilon}^{\rm in}\cdot\boldsymbol{\epsilon}^{\rm out})^2$. It is also shown that the Raman intensities of the D and 2D bands in strained graphene do not have a crystallographic orientation dependence in the bulk. At the edge, these

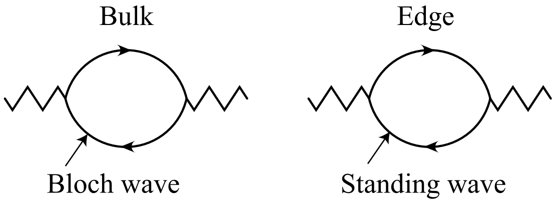

FIG. 3: Kohn anomaly effect at the bulk and edge. In the bulk, the intermediate electron-hole state consists of the Bloch plane wave, while at the edge, the intermediate state consists of the standing wave. The “spin” of the Bloch state can point arbitrary direction, while that of the standing wave can not have a component parallel to $\sigma_y \tau_z$.

bands can exhibit the polarization dependence similar to that of the G band and also have the crystallographic orientation dependence.

The off-diagonal term in Eq. (1), $\phi\sigma_x$ (or $\phi^*\sigma_x$), represents intervalley phonon modes which are responsible for the Raman D and 2D bands. Although the D and 2D bands consist of several phonon modes with different wave vectors which depend on the excitation laser energy, we examine the Kekulé distortion as the representative mode. It is straightforward to show that ϕ is a constant for Kekulé distortion, and $|\phi|$ is about three times larger than $|\mathbf{A}^{\rm q}|$ for the G band.[8] The latter can explain why the intensity of the 2D band is much larger than that of the G band. Let us denote $\phi = e^{i\theta}|\phi|$, then the el-ph interaction for the D band $H_{\rm D}$ is written by

$$H_{\rm D} = |\phi| \sigma_x \tau_\theta, \tag{30}$$

where $\tau_\theta \equiv \tau_x \cos\theta - \tau_y \sin\theta$. Because the matrices $\sigma_x\tau_x$ and $\sigma_x\tau_y$ do not appear in $\boldsymbol{v}$ and $\boldsymbol{v}^{\rm q}$, the D band can give us new information on the electronic structure that is not included in the G band. We will leave the phase θ of ϕ unspecified because θ relates to the TO modes near the Γ point through a gauge transformation as is shown in Sec. IV C.

A. D Band

The effective photon-phonon interaction for the Kekulé mode is written by

$$\mathcal{H}_{\rm D} \equiv |\phi| (\boldsymbol{\epsilon}^{\rm out} \cdot \boldsymbol{v}\sigma_z)^\dagger (\sigma_x \tau_\theta)(\boldsymbol{\epsilon}^{\rm in} \cdot \boldsymbol{v}\sigma_z). \tag{31}$$

It is easy to find that

$$\langle \mathcal{H}_{\rm D} \rangle \propto \boldsymbol{\epsilon}^{\rm in} \cdot \boldsymbol{\epsilon}^{\rm out} \langle \sigma_x \tau_\theta \rangle - i \boldsymbol{\epsilon}^{\rm in} \times \boldsymbol{\epsilon}^{\rm out} \langle \sigma_y \tau_{\theta + \frac{\pi}{2}} \rangle. \tag{32}$$

Hence, when $\boldsymbol{\epsilon}^{\rm in}$ is parallel with $\boldsymbol{\epsilon}^{\rm out}$, i.e., when $\boldsymbol{\epsilon}^{\rm in} \times \boldsymbol{\epsilon}^{\rm out} = 0$, the D band intensity is proportional to $|\langle \sigma_x \tau_\theta \rangle|^2$. On the other hand, when $\boldsymbol{\epsilon}^{\rm in}$ is perpendicular to $\boldsymbol{\epsilon}^{\rm out}$, i.e., $\boldsymbol{\epsilon}^{\rm in} \cdot \boldsymbol{\epsilon}^{\rm out} = 0$, the D band intensity is proportional to $|\langle \sigma_y \tau_{\theta+\frac{\pi}{2}} \rangle|^2$. If $|\langle \sigma_x \tau_\theta \rangle| \neq |\langle \sigma_y \tau_{\theta+\frac{\pi}{2}} \rangle|$, the D band intensity in the bulk can have a polarization dependence. However, we could not find any special reason for this asymmetry. Rather, it is probable that $|\langle \sigma_x \tau_\theta \rangle| = |\langle \sigma_y \tau_{\theta+\frac{\pi}{2}} \rangle|$ holds in the bulk. It is reasonable to consider that the D band intensity does not have a polarization dependence in the bulk.

Since the zigzag edge is not the source of intervalley scattering, we have $\langle \sigma_i \tau_x \rangle = 0$ and $\langle \sigma_i \tau_y \rangle = 0$ for the standing wave near the zigzag edge. Thus, we get

$$\langle H_{\rm D} \rangle = 0. \tag{33}$$

This shows that the D band intensity is suppressed near the zigzag edge. In contrast, the armchair edge is the source of intervalley scattering. In fact, the standing wave near the armchair edge is given by

$$\Psi_{\mathbf{k}}(\mathbf{r}) = C e^{ik_y y} \Phi_{\mathbf{k}} \begin{pmatrix} e^{+ik_x x} \\ e^{ia} e^{-ik_x x} \end{pmatrix}, \tag{34}$$

where C is normalization constant and $\Phi_{\mathbf{k}}$ is the wave function of the pseudospin.[9,14] It is easy to show that this wave function reproduces $\langle v_x \rangle = 0$ and $\langle v_y^{\rm q} \rangle = 0$, which is consistent with the results obtained in Sec. II. Moreover, pseudospin and valleyspin can be calculated separately since the armchair edge preserves the pseudospin. From Eq. (34), we get

$$\begin{aligned} \langle \sigma_x \tau_x \rangle &= \langle \sigma_x \rangle \cos(a - 2k_x x), \\ \langle \sigma_x \tau_y \rangle &= \langle \sigma_x \rangle \sin(a - 2k_x x). \end{aligned} \tag{35}$$

By using these results, we obtain

$$\langle H_{\rm D} \rangle = |C|^2 \int_S |\phi| \langle \sigma_x \rangle \cos\left(\theta + a - 2k_x x\right) dx dy, \tag{36}$$

for the armchair edge. To summarize, the D band has an obvious selection rule; the D band is Raman active at the armchair edge while it is not active at the zigzag edge. This has been a well-known fact which is useful in distinguishing armchair-dominated edge from zigzag-dominated edge.[7,10–12]

The polarization dependence of the D band intensity near the armchair edge is different from that in the bulk. In fact, we get from $\langle \mathcal{H}'_{\rm D} \rangle \equiv |\phi| \langle \boldsymbol{\epsilon}^{\rm out} \cdot \boldsymbol{v}\sigma_z \rangle^\dagger \langle \sigma_x \tau_\theta \rangle \langle \boldsymbol{\epsilon}^{\rm in} \cdot \boldsymbol{v}\sigma_z \rangle$ that

$$\langle \mathcal{H}'_{\rm D} \rangle \propto |\phi| \epsilon_y^{\rm in} \epsilon_y^{\rm out} \langle v_x^{\rm q} \rangle^3. \tag{37}$$

Let the angle between the armchair edge and the polarization of the incident (scattered) laser be $\Theta_{\rm in}$ ($\Theta_{\rm out}$). Then we can use $\epsilon_y^{\rm in} = \epsilon^{\rm in} \cos\Theta_{\rm in}$ and $\epsilon_y^{\rm out} = \epsilon^{\rm out} \cos\Theta_{\rm out}$ in Eq. (37). Thus, the D band intensity at the armchair edge behaves according to $I_{\rm D} \propto \cos^2\Theta_{\rm in} \cos^2\Theta_{\rm out}$ which is maximum when the polarization of the incident (or scattered) light is parallel to the edge.

Here, let us mention experiments on the polarization dependence for the D band intensity at the edge. First, the polarization dependence of $I_{\rm D} \propto \cos^2\Theta_{\rm in} \cos^2\Theta_{\rm out}$ is consistent with the observation for graphite edges by

Cançado *et al.*[10,30] and the observations for edges of single-layer graphene by You *et al.*[11], Gupta *et al.*[12] and Casiraghi *et al.*[31] Secondly, for edges of single-layer graphene, Cong *et al.*[15] confirmed that not only the D band but also the G band follows $I_{\rm D,G} \propto \cos^2\Theta_{\rm in}$ for the polarization of the incident laser light, whereas You *et al.*[11] and Gupta *et al.*[12] did not observe any polarization dependence for the G band. On the other hand, for edges of bilayer graphene, Begliarbekov *et al.*[16] showed that the G band intensity had the polarization dependence, while the D band intensity did not exhibit any polarization dependence. The polarization dependence of the D band at the armchair edge might be sensitive to the number of graphene layers. In fact, Gupta *et al.*[12] shows that three Lorentzian components are necessary to fit the Raman spectrum of the D band in bilayer graphene, whereas the D band spectra in a single-layer graphene can be well fitted by a single Lorentzian component. Theoretically, by comparing Eq. (37) with Eq. (26), we see that the polarization dependence of the D band intensity at the armchair edge is identical to that of the G band intensity at the armchair edge. We also note that when zigzag and armchair edges are randomly distributed along a mixed edge, the G band does not show a polarization dependence.[14] However, even in this case, the D band should have a polarization dependence since there is no counterpart of the D band which can erase the polarization dependence. In the case of the G band, two components (LO and TO modes) can coexist in the random edge. They have different polarization dependence, so that a polarization dependence of the G band may diminish in the case of a random edge.

Equation (37) leads to the following polarization dependence on the crystallographic orientation in strained graphene,

$$I_{\rm D} \propto \sin^2(\theta_{\rm in} + \varphi_s)\sin^2(\theta_{\rm out} + \varphi_s). \tag{38}$$

Thus, from Eq. (27) we find that $I_{\rm D} \propto I_{\rm G^+} + I_{\rm G^-}$. This might be one of the most interesting consequence for the G and D bands concerning with the armchair edge in strained graphene.

B. 2D Band

The effective el-ph interaction for the 2D band is given by the square of $H_{\rm D}$ as

$$H_{\rm 2D} = H_{\rm D}^2 = |\phi|^2\sigma_0\tau_0. \tag{39}$$

Because the effective interaction is proportional to the identity matrix $\sigma_0\tau_0$, no constraint can affect the el-ph matrix element for the 2D band. The effective photon-phonon interaction for the 2D band in the bulk is given by

$$\mathcal{H}_{\rm 2D} \equiv (\boldsymbol{\epsilon}^{\rm out}\cdot\boldsymbol{v}\sigma_z)^\dagger(|\phi|^2\sigma_0\tau_0)(\boldsymbol{\epsilon}^{\rm in}\cdot\boldsymbol{v}\sigma_z). \tag{40}$$

Then we have

$$\langle\mathcal{H}_{\rm 2D}\rangle \propto (\boldsymbol{\epsilon}^{\rm in}\cdot\boldsymbol{\epsilon}^{\rm out})\sigma_0\tau_0 - i(\boldsymbol{\epsilon}^{\rm in}\times\boldsymbol{\epsilon}^{\rm out})\sigma_z\tau_z. \tag{41}$$

Note that $\langle\sigma_0\tau_0\rangle = 1$ holds for any kind of wave function. Furthermore, the condition $\langle\sigma_z\tau_z\rangle = 0$ should be satisfied in the absence of a magnetic field.[8] Consequently, the 2D band intensity follows $I_{\rm 2D} \propto (\boldsymbol{\epsilon}^{\rm in}\cdot\boldsymbol{\epsilon}^{\rm out})^2$ in the absence of a magnetic field. The Raman intensity of the 2D band in bulk is maximum when the incident and scattered polarizations are parallel and minimum when they are orthogonal, which is in good agreement with the experimental result by Yoon *et al.*[32] The polarization dependence of the 2D band closely resembles that of Rayleigh scattering[33] because the effective Hamiltonian for Rayleigh scattering is given by

$$\mathcal{H}_{\rm R} \equiv e^2(\boldsymbol{\epsilon}^{\rm out}\cdot\boldsymbol{v}\sigma_z)^\dagger(\boldsymbol{\epsilon}^{\rm in}\cdot\boldsymbol{v}\sigma_z). \tag{42}$$

Note that $\mathcal{H}_{\rm R}$ is the same as $\mathcal{H}_{\rm 2D}$ except for the numerical factor (coupling constant). In contrast, for the edge, the polarization dependence of the 2D band intensity is the same as that of the D band:

$$\langle\mathcal{H}'_{\rm 2D}\rangle \propto |\phi|^2\epsilon_y^{\rm in}\epsilon_y^{\rm out}\langle v_x^{\rm q}\rangle^2. \tag{43}$$

Note, however, that because the el-ph matrix element for the 2D band is given by $\langle H_{\rm 2D}\rangle = |\phi|^2$ regardless of the orientation of the edge, the 2D band intensity appears both at the zigzag and armchair edges. The constraint works for the optical transition only, and therefore the polarization dependence of the 2D band follows the same rule for the G band.

It is known that Eq. (30) does not cover the deformations representing a pentagon or heptagon.[34,35] For these topological defects, some combination of $\sigma_a\tau_b$ besides $\sigma_x\tau_x$ and $\sigma_x\tau_y$ can appear. Thus, besides the appearance of the Raman peak due to the vibrational dynamics specific to the topological defect,[36] the D and 2D bands can have some information on the presence of the topological defect. In fact, it is known that a single pentagon or a single heptagon gives rise to a mixing between K and K′ points, leading to a sophisticated topological effect on the wave function. Recently, the existence of a new type of graphene edge called reczag (reconstructed zigzag) has been proposed.[37] Note that this reczag edge consists of a pair of pentagon and heptagon along the edge. In this case, the topological effect on the wave function is not significant because the topological effect of a single pentagon is cancelled by that of a single heptagon. In fact, a numerical calculation shows the appearance of the edge states near the reczag edge.[38] This indicates that the standing wave near the reczag edge is similar to that near the usual zigzag edge.

C. Gauge Transformation and D′ Band

At first sight, due to the momentum conservation, a TO mode with small nonzero momentum ($\mathbf{q} \neq 0$ and

$|\mathbf{q}| \ll |\mathbf{k}_{\rm F}|$) may cause an intravalley scattering, but is not expected to be relevant to an intervalley scattering. Here, in terms of the gauge transformation, we shall show that such TO modes do not contribute to intravalley scattering; rather they can be activated through the intervalley scattering.

The TO modes with small momentum can be represented by the derivative of some scalar function $\varphi(\mathbf{r})$ as

$$\mathbf{A}^{\rm q}_{\rm TO}(\mathbf{r}) = \mathbf{A}^{\rm q}_{\rm TO} + \nabla\varphi(\mathbf{r}), \tag{44}$$

where $\mathbf{A}^{\rm q}_{\rm TO}$ on the right-hand side is the zero mode which has been relevant to the G band.[39] Due to the following gauge transformation, the scalar function can be transferred to the phases of the wave function and ϕ as

$$\begin{pmatrix} \boldsymbol{\sigma}\cdot(\hat{\mathbf{p}} + \mathbf{A}^{\rm q}_{\rm TO}) & \tilde{\phi}\sigma_x \\ \tilde{\phi}^*\sigma_x & \boldsymbol{\sigma'}\cdot(\hat{\mathbf{p}} - \mathbf{A}^{\rm q}_{\rm TO}) \end{pmatrix} \begin{pmatrix} \tilde{\Psi}_{\rm K} \\ \tilde{\Psi}_{\rm K'} \end{pmatrix}, \tag{45}$$

where $\tilde{\Psi}_{\rm K} = e^{-i\varphi(\mathbf{r})}\Psi_{\rm K}$, $\tilde{\Psi}_{\rm K'} = e^{+i\varphi(\mathbf{r})}\Psi_{\rm K'}$, and $\tilde{\phi} = e^{-2i\varphi(\mathbf{r})}\phi$. Note that the TO mode appears as the phase of ϕ (see θ in Eq. (30)). A physical significant of this gauge transformation is that the TO mode can be excited in combination with the intervalley scattering. Since the armchair edge enhances the intervalley scattering ϕ, the TO mode with small nonzero momentum $\varphi(\mathbf{r})$ also can be excited near the armchair edge.

The LO modes with small momentum can be represented by the derivative of some scalar function $\chi(\mathbf{r})$ as

$$\mathbf{A}^{\rm q}_{\rm LO}(\mathbf{r}) = \mathbf{A}^{\rm q}_{\rm LO} + \nabla\times(\chi(\mathbf{r})\mathbf{e}_z). \tag{46}$$

In contrast to the TO mode, $\mathbf{A}^{\rm q}_{\rm LO}(\mathbf{r})$ can not be gauge transformed into the phase of ϕ because it has a non-vanishing field strength: $B^{\rm q}_z = \nabla\times\mathbf{A}^{\rm q}_{\rm LO}(\mathbf{r}) \neq 0$.[20] Thus, these LO modes are responsible for intravalley scattering. The D′ band[40] observed slightly above the G band in Raman spectra (around 1620cm^{-1}) is originated from these LO modes. The Hamiltonian for the D′ band is given by

$$H_{\rm D'} = \mathbf{A}^{\rm q}(\mathbf{r})\cdot\boldsymbol{v}^{\rm q}. \tag{47}$$

Note that the "spin" structure is the same as that for the G band. Thus, the polarization dependence of the D′ band follows that of the G band in the bulk. At edge, we have $\langle H_{\rm D'}\rangle = \int_S A^{\rm q}_x(\mathbf{r})\Psi^\dagger(\mathbf{r})v^{\rm q}_x\Psi(\mathbf{r})dxdy$. The intensity behaves as $I_{\rm D'} \propto |\epsilon^{\rm out}_y\epsilon^{\rm in}_y|^2$. The polarization dependence of the D′ band is the same as that of the G band at edge, however, it might be difficult to observe the polarization dependence of $I_{\rm D'}$ due to its small intensity.

V. DISCUSSION AND SUMMARY

Here, we would like to mention the status of the experiment on the G band for the graphene edge. Cong *et al.*[15] conducted a systematic research on edges of single layer graphene and found, in particular, that there were two orientations of the graphene edge (A-edge and Z-edge) which exhibited different behaviors against the polarization of the incident laser light. The Raman intensity of the A-edge ($I_{\rm A}$) is enhanced when the polarization becomes parallel to the edge and that of the Z-edge ($I_{\rm Z}$) is enhanced when the polarization becomes perpendicular to the edge. By using the angle Θ between the orientation of the edge and the polarization of the incident laser light, they could fit the observed Raman intensities $I_{\rm A}(\Theta)$ and $I_{\rm Z}(\Theta)$ with

$$\begin{aligned} I_{\rm A}(\Theta) &= a + b\cos^2\Theta, \\ I_{\rm Z}(\Theta) &= c + d\sin^2\Theta, \end{aligned} \tag{48}$$

where a, b, c, and d are fitting parameters. In their experimental data, the maximum intensity ($a+b$ or $c+d$) is about two times larger than the minimum intensity (a or c), so that $a/(a+b)$ and $c/(c+d)$ is about $1/2$.

The appearance of these two behaviors for the G band is consistent with the selection rule at the graphene edge.[14] The A-edge is considered to be armchair dominant edge and the Z-edge is zigzag dominant edge. The ratio of the minimum intensity to the maximum intensity corresponds to the square of the ratio of the zigzag (armchair) part to the armchair (zigzag) part in a mixed edge.[14] We thus estimate that the A-edge consists of 60% armchair and 40% zigzag edge, while the Z-edge consists of 40% armchair and 60% zigzag edge. We can get the similar value for the data obtained by Begliarbekov *et al.*[16] who carried out polarization resolved micro-Raman spectroscopy at edges of bilayer graphene. The two orientations (A-edge and Z-edge) were clearly resolved even in bilayer graphene, which also suggests that the number of graphene layers does not invalidate the selection rule for the G band. Cançado *et al.*[30] observed that the Raman intensity of the G band for a nanoribbon located on top of a highly oriented pyrolytic graphite (HOPG) has a strong dependence on the incident light polarization. They showed that the Raman intensity is maximum when the polarization is parallel to the edge of a nanoribbon. Their result is consistent with the selection rule for the armchair edge. A notable point in their experiment is that the ratio of the maximum intensity to the minimum intensity was very high. We speculate that the nanoribbon located on top of HOPG had rather regular armchair edge.

At this moment, we do not know how to make a clear distinction between bulk and edge. In other words, there exists no criteria by which we can decide whether the Raman process is best described by $\langle\mathcal{H}_{\rm G}\rangle$ (Eq. (19)) or $\langle\mathcal{H}'_{\rm G}\rangle$ (Eq. (25)). Since the electron dynamics in graphene is given by massless Dirac equation which is a scale-less theory, we consider that bulk of graphene can not be completely separated from the edge. To put it in an extreme way, there is no bulk region in a nanoribbon with perfect regular edge, as well as that there is no edge region in a nanotube. The problem is the case of a mixed rough edge which might bring a characteristic length scale to

TABLE I: Polarization dependences of the Raman intensities for the optical phonon modes in strained graphene. × represents absence of a polarization dependence. For "Bulk", $\theta_{\rm in}$ ($\theta_{\rm out}$) denotes the angle between the strain and the incident (scattered) laser polarization, and φ_s is the angle between the direction of strain and the zigzag edge (x-axis). For the "Armchair" and "Zigzag" edges, $\Theta_{\rm in}$ ($\Theta_{\rm out}$) denotes the angle between the incident (scattered) laser polarization and the armchair or zigzag edge. The polarization dependence of the G band Raman intensity in unstrained graphene is given by $I_{G^+} + I_{G^-}$, so that the polarization dependence on the crystallographic orientation of strained graphene is lost at the bulk.

	G^+	G^-	D	2D (G′)
Bulk	$\cos^2(\theta_{\rm in}+\theta_{\rm out}+\varphi_s)$	$\sin^2(\theta_{\rm in}+\theta_{\rm out}+\varphi_s)$	×	$(\boldsymbol{\epsilon}^{\rm in}\cdot\boldsymbol{\epsilon}^{\rm out})^2$
Armchair	$\cos^2(\varphi_s)\cos^2(\Theta_{\rm in})\cos^2(\Theta_{\rm out})$	$\sin^2(\varphi_s)\cos^2(\Theta_{\rm in})\cos^2(\Theta_{\rm out})$	$\cos^2(\Theta_{\rm in})\cos^2(\Theta_{\rm out})$	$\cos^2(\Theta_{\rm in})\cos^2(\Theta_{\rm out})$
Zigzag	$\cos^2(\varphi_s)\sin^2(\Theta_{\rm in})\sin^2(\Theta_{\rm out})$	$\sin^2(\varphi_s)\sin^2(\Theta_{\rm in})\sin^2(\Theta_{\rm out})$	×	$\sin^2(\Theta_{\rm in})\sin^2(\Theta_{\rm out})$

the scale-less theory. Theoretical estimation of the effective length is an important issue should be carried out in the near future. Experimentally, according to the Raman mapping data by Cong *et al.*,[15] the effective region from the edge in which the description using the standing wave is valid, is about 400 nm, which seems to be comparable to the Gaussian laser beam waist.[12]

Let us investigate the property of an eigenstate in the interior part of graphene. Since a graphene has the edge, the electronic wave function is given by the standing wave. Furthermore, the expectation value of the velocity, $\langle \boldsymbol{v} \rangle$, must vanish, so that we have $\langle v_x \rangle = 0$ and $\langle v_y \rangle = 0$ for the standing wave. Note that in the case of nanotubes the velocity around the axis of the tube takes nonzero value in general. Suppose that the graphene is surrounded by the zigzag edges only [See Fig. 2(b,top)]. Then, $\langle v_x \rangle = 0$ and $\langle v_y \rangle = 0$ must be satisfied at each valley since the zigzag edge is not the source of intervalley scattering. Because the velocity and the axial velocity are related with each other by $\boldsymbol{v}^{\rm q} = \boldsymbol{v}\tau_z$, we have $\langle \boldsymbol{v}^{\rm q} \rangle = 0$. It is amusing to note that in this special case Eq. (23) suggests that the resonant G band intensity vanishes. In contrast, when graphene is surrounded by the armchair edges only [See Fig. 2(b,bottom)], we have $\langle v_x^{\rm q} \rangle \neq 0$ and $\langle v_y^{\rm q} \rangle = 0$ since the armchair edge is relevant (irrelevant) to the valleyspin (pseudospin). Note that in both hexagonal graphenes, we have at least the condition $\langle v_y^{\rm q} \rangle = 0$. It is our speculation based on the observation of several edge shapes that the constraint $\langle v_y^{\rm q} \rangle = 0$ holds for graphene with a wider variety of edge shapes.

The formalism using the gauge fields for photon $\mathbf{A}$ and phonon $\mathbf{A}^{\rm q}$ might provide a new and fresh insight into Raman scattering, which otherwise well-studied subject. In ordinary Raman spectroscopy, we irradiate a laser light $\mathbf{A}^{\rm in}$ onto a graphene sample and observe the inelastically scattered light $\mathbf{A}^{\rm out}$. This Raman process in unstrained graphene may be represented as

$$\mathbf{A}^{\rm in} \to \mathbf{A}^{\rm q} + \mathbf{A}^{\rm out}. \tag{49}$$

The left-hand side of "→" shows the input and the right-hand side of it denotes the output. Note that a phonon $\mathbf{A}^{\rm q}$ on the right-hand side is a kind of lattice deformation or an internal strain. Thus, in Raman spectroscopy, by inputting a photon (electronic) signal, one gets a signal of strain from graphene. Let us consider a process represented by

$$\mathbf{A}^{\rm q}_{\rm in} \to \mathbf{A} + \mathbf{A}^{\rm q}_{\rm out}, \tag{50}$$

where $\mathbf{A}^{\rm q}$ represents an external strain. This process of Eq. (50) is given by replacing $\mathbf{A}$ ($\mathbf{A}^{\rm q}$) with $\mathbf{A}^{\rm q}$ ($\mathbf{A}$) in Eq. (49). In this process, by inputting strain, one gets an electronic output $\mathbf{A}$ from graphene, which seems to be a prototypical process of strain engineering. Now, the Raman process in strained graphene[17,18,41–45] is expressed by

$$\mathbf{A}^{\rm q}_{\rm bulk} + \mathbf{A}^{\rm in} \to \mathbf{A}^{\rm q}_{\rm bulk} + \mathbf{A}^{\rm q} + \mathbf{A}^{\rm out}, \tag{51}$$

where the strain is described by $\mathbf{A}^{\rm q}_{\rm bulk}$. Considering that this is a process which may be recognized as the sum of Eqs. (49) and (50), it can be said that Raman spectroscopy in strained graphene is a small step toward strain engineering in graphene.

It is reasonable to consider that Eq. (49) represents a Raman process in graphene without edge. Strictly speaking, a Raman process in a real (unstrained) graphene should be represented not by Eq. (49) but by

$$\mathbf{A}^{\rm q}_{\rm edge} + \mathbf{A}^{\rm in} \to \mathbf{A}^{\rm q}_{\rm edge} + \mathbf{A}^{\rm q} + \mathbf{A}^{\rm out}, \tag{52}$$

because the presence of the edge is represented by a local strain field $\mathbf{A}^{\rm q}_{\rm edge}$: the zigzag edge is represented by a local $\mathbf{A}^{\rm q}$ field parallel to the edge, while the armchair edge corresponds to a local $\mathbf{A}^{\rm q}$ field normal to the edge.[9,46] It is interesting to note that the direction of the $\mathbf{A}^{\rm q}_{\rm edge}$ is coincident with that of the Raman active phonon mode $\mathbf{A}^{\rm q}$ near the graphene edge. Considering that $\mathbf{A}^{\rm q}_{\rm bulk}$ in Eq. (51) ($\mathbf{A}^{\rm q}_{\rm edge}$ in Eq. (52)) represents a global (local) strain, the Raman spectroscopy near the graphene edge[10–12,15,16] is complementary to the Raman spectroscopy in the bulk of strained graphene.

In conclusion, the polarization dependences of the G, D, and 2D Raman bands at bulk and edge have been investigated theoretically with paying attention to the pseudospin and valleyspin of the standing wave. Our results are summarized in TABLE I. The constraint for the axial velocity provided by the graphene edge is essential to the selection rule for each Raman band. The selection rules of the G and D bands for graphene edge are consistent with the recent experimental results. The coherence provided by the graphene edge seems to persist even in the bulk, by which we explain the recent experiments for strained graphene showing the crystallographic orientation dependences of the Raman intensities of the G^+ and G^- bands. This also suggests that the "bulk" of graphene can not be completely free from the surrounding graphene edge, and that it is necessary to distinguish the bulk of graphene that is surrounded by edge from the bulk of a periodic graphene without edge.

Acknowledgments

K.S. would like to thank P. Kim, C. Cong, and T. You. This work was motivated by the discussion with them. He also wishes to thank S. Mathew for useful discussions. This work is supported by a Grant-in-Aid for Specially Promoted Research (No. 20001006) from the Ministry of Education, Culture, Sports, Science and Technology (MEXT).

---

[*] Email address: SASAKI.Kenichi@nims.go.jp

[1] M. S. Dresselhaus, A. Jorio, M. Hofmann, G. Dresselhaus, and R. Saito, Nano Lett. **10**, 751 (2010).

[2] D. Graf, F. Molitor, K. Ensslin, C. Stampfer, A. Jungen, C. Hierold, and L. Wirtz, Nano Lett. **7**, 238 (2007).

[3] A. C. Ferrari, J. C. Meyer, V. Scardaci, C. Casiraghi, M. Lazzeri, F. Mauri, S. Piscanec, D. Jiang, K. S. Novoselov, S. Roth, et al., Phys. Rev. Lett. **97**, 187401 (2006).

[4] Z. H. Ni, H. M. Wang, J. Kasim, H. M. Fan, T. Yu, Y. H. Wu, Y. P. Feng, and Z. X. Shen, Nano Lett. **7**, 2758 (2007).

[5] C. Thomsen and S. Reich, Phys. Rev. Lett. **85**, 5214 (2000).

[6] R. Saito, A. Gruneis, G. G. Samsonidze, V. W. Brar, G. Dresselhaus, M. S. Dresselhaus, A. Jorio, L. G. Cancado, C. Fantini, M. A. Pimenta, et al., New J. Phys. **5**, 157 (2003).

[7] L. Malard, M. Pimenta, G. Dresselhaus, and M. Dresselhaus, Phys. Rep. **473**, 51 (2009).

[8] K. Sasaki and R. Saito, Prog. Theor. Phys. Suppl. **176**, 253 (2008).

[9] K. Sasaki and K. Wakabayashi, Phys. Rev. B **82**, 035421 (2010).

[10] L. G. Cançado, M. A. Pimenta, B. R. A. Neves, M. S. S. Dantas, and A. Jorio, Phys. Rev. Lett. **93**, 247401 (2004).

[11] Y. You, Z. Ni, T. Yu, and Z. Shen, Appl. Phys. Lett. **93**, 163112 (2008).

[12] A. K. Gupta, T. J. Russin, H. R. Gutierez, and P. C. Eklund, ACS Nano **3**, 45 (2009).

[13] K. Sasaki, M. Yamamoto, S. Murakami, R. Saito, M. Dresselhaus, K. Takai, T. Mori, T. Enoki, and K. Wakabayashi, Phys. Rev. B **80**, 155450 (2009).

[14] K. Sasaki, R. Saito, K. Wakabayashi, and T. Enoki, J. Phys. Soc. Jpn. **79**, 044603 (2010).

[15] C. Cong, T. Yu, and H. Wang, ACS Nano **4**, 3175 (2010).

[16] M. Begliarbekov, O. Sul, S. Kalliakos, E.-H. Yang, and S. Strauf, Appl. Phys. Lett. **97**, 031908 (2010).

[17] M. Huang, H. Yan, C. Chen, D. Song, T. F. Heinz, and J. Hone, Proceedings of the National Academy of Sciences **106**, 7304 (2009).

[18] T. M. G. Mohiuddin, A. Lombardo, R. R. Nair, A. Bonetti, G. Savini, R. Jalil, N. Bonini, D. M. Basko, C. Galiotis, N. Marzari, et al., Phys. Rev. B **79**, 205433 (2009).

[19] C. L. Kane and E. J. Mele, Phys. Rev. Lett. **78**, 1932 (1997).

[20] K. Sasaki, Y. Kawazoe, and R. Saito, Prog. Theor. Phys. **113**, 463 (2005).

[21] M. Katsnelson and A. Geim, Phil. Trans. R. Soc. A **366**, 195 (2008).

[22] E. McCann and V. I. Fal'ko, Journal of Physics: Condensed Matter **16**, 2371 (2004).

[23] A. R. Akhmerov and C. W. J. Beenakker, Phys. Rev. B **77**, 085423 (2008).

[24] K. Sasaki, K. Wakabayashi, and T. Enoki, New J. Phys. **12**, 083023 (2010).

[25] O. Dubay, G. Kresse, and H. Kuzmany, Phys. Rev. Lett. **88**, 235506 (2002).

[26] K. Ishikawa and T. Ando, J. Phys. Soc. Jpn. **75**, 084713 (2006).

[27] M. Lazzeri and F. Mauri, Phys. Rev. Lett. **97**, 266407 (2006).

[28] T. Ando, J. Phys. Soc. Jpn. **75**, 124701 (2006).

[29] J. Yan, Y. Zhang, P. Kim, and A. Pinczuk, Phy. Rev. Lett. **98**, 166802 (2007).

[30] L. G. Cançado, M. A. Pimenta, B. R. A. Neves, G. Medeiros-Ribeiro, T. Enoki, Y. Kobayashi, K. Takai, K.-i. Fukui, M. S. Dresselhaus, R. Saito, et al., Phys. Rev. Lett. **93**, 47403 (2004).

[31] C. Casiraghi, A. Hartschuh, H. Qian, S. Piscanec, C. Georgi, A. Fasoli, K. S. Novoselov, D. M. Basko, and A. C. Ferrari, Nano Lett. **9**, 1433 (2009).

[32] D. Yoon, H. Moon, Y.-W. Son, G. Samsonidze, B. H. Park, J. B. Kim, Y. Lee, and H. Cheong, Nano Lett. **8**, 4270 (2008).

[33] C. Casiraghi, A. Hartschuh, E. Lidorikis, H. Qian, H. Harutyunyan, T. Gokus, K. S. Novoselov, and A. C. Ferrari, Nano Lett. **7**, 2711 (2007).

[34] J. González, F. Guinea, and M. A. H. Vozmediano, Phys.

Rev. Lett. **69**, 172 (1992).

[35] P. E. Lammert and V. H. Crespi, Phys. Rev. Lett. **85**, 5190 (2000).

[36] T. E. Doyle and J. R. Dennison, Phys. Rev. B **51**, 196 (1995).

[37] P. Koskinen, S. Malola, and H. Häkkinen, Phys. Rev. B **80**, 073401 (2009).

[38] P. Koskinen, S. Malola, and H. Häkkinen, Phys. Rev. Lett. **101**, 115502 (2008).

[39] K. Sasaki, R. Saito, G. Dresselhaus, M. S. Dresselhaus, H. Farhat, and J. Kong, Phys. Rev. B **77**, 245441 (2008).

[40] R. Saito, A. Jorio, A. G. Souza Filho, G. Dresselhaus, M. S. Dresselhaus, and M. A. Pimenta, Phys. Rev. Lett. **88**, 027401 (2001).

[41] Z. H. Ni, T. Yu, Y. H. Lu, Y. Y. Wang, Y. P. Feng, and Z. X. Shen, ACS Nano **2**, 2301 (2008).

[42] T. Yu, Z. Ni, C. Du, Y. You, Y. Wang, and Z. Shen, J. Phys. Chem. C **112**, 12602 (2008).

[43] G. Tsoukleri, J. Parthenios, K. Papagelis, R. Jalil, A. C. Ferrari, A. K. Geim, K. S. Novoselov, and C. Galiotis, Small **5**, 2397 (2009).

[44] J. A. Robinson, C. P. Puls, N. E. Staley, J. P. Stitt, M. A. Fanton, K. V. Emtsev, T. Seyller, and Y. Liu, Nano Lett. **9**, 964 (2009).

[45] O. Frank, G. Tsoukleri, J. Parthenios, K. Papagelis, I. Riaz, R. Jalil, K. S. Novoselov, and C. Galiotis, ACS Nano **4**, 3131 (2010).

[46] K. Sasaki, S. Murakami, and R. Saito, J. Phys. Soc. Jpn. **75**, 074713 (2006).

[47] D. M. Basko, Phys. Rev. B **79**, 129902 (2009).

[48] In the case of Γ point phonon, the definitions of the LO and TO modes are not unique since we do not have any reference vector. It seems standard that the LO mode is taken as the mode parallel with respect to the edge and the TO mode is the one perpendicular to the edge.

[49] A similar equation was derived by Basko.[47] Note, however, that Eq. (20) is different from Eq. (53) in Ref. 47 as the former contains the axial velocity $v_i^{\rm q}$, while the latter does not. Due to $v_i^{\rm q}$, Eq. (20) is symmetric with respect to the change of x and y. The existence of $v_i^{\rm q}$ in Eq. (20) is essential in the subsequent arguments.

[50] In literature, $3\varphi_s$ instead of φ_s appears in the angle Ψ. The factor of 3 in front of φ_s seems to come from the choice of the coordinate system, for which φ_s in Eq. (21) is replaced with $-\varphi_s$.[18] We could not find any proper reason for this choice.

[51] This feature of graphene bulk is different from that of nanotube because the electronic dispersion is not isotropic in the case of nanotube due to the cutting lines.